



来自夸克-胶子等离子体的弱磁辐射

孙静安 严力

**The Weak Magnetic Photon Emission from Quark-gluon Plasma**

SUN Jing' an, YAN Li

在线阅读 View online: <https://doi.org/10.11804/NuclPhysRev.41.2023CNPC14>

引用格式:

孙静安, 严力. 来自夸克-胶子等离子体的弱磁辐射[J]. *原子核物理评论*, 2024, 41(1):558-563. doi: 10.11804/NuclPhysRev.41.2023CNPC14

SUN Jing' an, YAN Li. The Weak Magnetic Photon Emission from Quark-gluon Plasma[J]. *Nuclear Physics Review*, 2024, 41(1):558-563. doi: 10.11804/NuclPhysRev.41.2023CNPC14

---

您可能感兴趣的其他文章

Articles you may be interested in

[GeV能区碰撞中正反质子椭圆流劈裂的研究](#)

Investigation of the Splitting in Elliptic Flow Between Protons and Anti-protons in + Collisions at  
原子核物理评论. 2020, 37(3): 660-667 <https://doi.org/10.11804/NuclPhysRev.37.2019CNPC04>

[强磁场与涡旋场中的夸克胶子物质](#)

Quark Gluon Matter in Strong Magnetic and Vortical Fields

原子核物理评论. 2020, 37(3): 414-425 <https://doi.org/10.11804/NuclPhysRev.37.2019CNPC29>

[动量相关势对直接流和椭圆流的影响](#)

The Influence of the Momentum Dependence Potential on the Directed Flow and Elliptic Flow

原子核物理评论. 2022, 39(1): 16-22 <https://doi.org/10.11804/NuclPhysRev.39.2021071>

[相对论重离子对撞机上重味衰变电子的测量数据中粲和底成分的分](#)

Charm and Beauty Separation from Heavy Flavor Electron Measurements at RHIC

原子核物理评论. 2020, 37(3): 684-689 <https://doi.org/10.11804/NuclPhysRev.37.2019CNPC13>

[强电场对夸克胶子等离子体中粲夸克偶素演化的影响\(英文\)](#)

Effect of Strong Electric Field on the Evolution of Charmonium in Quark Gluon Plasma

原子核物理评论. 2019, 36(3): 278-288 <https://doi.org/10.11804/NuclPhysRev.36.03.278>

[基于中能重离子碰撞研究高密对称能](#)

Probing High-density Symmetry Energy Using Heavy-ion Collisions at Intermediate Energies

原子核物理评论. 2020, 37(2): 136-150 <https://doi.org/10.11804/NuclPhysRev.37.2019068>

Article ID: 1007-4627(2024)01-0558-06

# The Weak Magnetic Photon Emission from Quark-gluon Plasma

SUN Jing'an<sup>1</sup>, YAN Li<sup>1,2,†</sup>

(1. Institute of Modern Physics, Fudan University, Shanghai 200433, China;

2. Key Laboratory of Nuclear Physics and Ion-beam Application (MOE), Fudan University, Shanghai 200433, China)

**Abstract:** There must be electromagnetic fields created during high-energy heavy-ion collisions. Although the electromagnetic field may become weak with the evolution of the quark-gluon plasma (QGP), compared to the energy scales of the strong interaction, they are potentially important to some electromagnetic probes. In this work, we propose the coupled effect of the weak magnetic field and the longitudinal dynamics of the background medium for the first time. We demonstrate that the induced photon spectrum can be highly azimuthally anisotropic when the quark-gluon plasma is in the presence of a weak external magnetic field. On the other hand, the weak magnetic photon emission from quark-gluon plasma only leads to a small correction to the photon production rate. After hydrodynamic evolution with a tilted fireball configuration, the experimentally measured direct photon elliptic flow is well reproduced. Meanwhile, the used time-averaged magnetic field in the hydrodynamic stage is found no larger than a few percent of the pion mass square.

**Key words:** heavy-ion collision; the direct photon; weak magnetic field; elliptic flow

**CLC number:** O571.53    **Document code:** A    **DOI:** 10.11804/NuclPhysRev.41.2023CNPC14

## 0 Introduction

In high-energy heavy-ion experiments carried out at the Relativistic Heavy-Ion Collider (RHIC) and the Large Hadron Collider (LHC), a novel state of matter, known as quark-gluon plasma (QGP), has been created, which with quark and gluon degrees of freedom<sup>[1]</sup>. Studying the dynamic properties of QGP is an important means to enhance our understanding of quantum chromodynamics (QCD)<sup>[2]</sup>. It has been established that QGP behaves as a perfect fluid theoretically, and viscous hydrodynamics has been proven to be a remarkably successful model that can account for many experimental observables related to charged hadrons<sup>[3-4]</sup>.

As penetrating probes, photons have a large mean-free path in the quark-gluon plasma. They are emitted immediately after their production and provide information about the system, rendering them a more direct means of studying the properties of QGP<sup>[5-7]</sup>. Unfortunately, the hydrodynamic model fails to reproduce the photon spectrum. At the top RHIC energies, in the low  $p_T$  region, experimentally measured direct photon yields (*i.e.*, photon yields excluding those from hadron decays) exceed the current theoretical predictions. In particular, it has been found that direct photons exhibit a large elliptic flow  $v_2$ , comparable to

that of pions<sup>[8-11]</sup>. However, according to theoretical expectations, the direct photons should be isotropic because they are dominantly from the early stages, where the momentum anisotropy has not been fully developed. The observation of the yield excess and the large elliptic flow of direct photons, which contradicts theoretical expectations, is often referred to as "the direct photon puzzle"<sup>[12-15]</sup>.

Incorporating a significant emission anisotropy for the direct photons in hydrodynamic models is challenging. In the most updated multi-messenger calculation focusing on direct photons<sup>[13]</sup>, many ingredients have been taken into account: (i) the photon emission from the pre-equilibrium stage based on KoMPost is considered; (ii) the quark chemical equilibration time is also studied; (iii) the updated next-next leading order perturbative QCD is used for prompt photons; and (iv) the distribution functions with shear and bulk viscous corrections are used to calculate the photon emission rate. However, the yield excess at the low  $p_T$  region is still notable. More importantly, the  $v_2^{\gamma}$  is still under-predicted.

The presence of a magnetic field provides a possible solution to the direct photon puzzle. In high-energy heavy-ion collisions, as a consequence of the relativistic motion of ions, magnetic fields are generated with extremely strong field strength, with  $|eB| \approx 10m_{\pi}^2$  at the top energies of

Received date: 29 Jun. 2023;    Revised date: 06 Jan. 2024

Foundation item: National Natural Science Foundation of China (11975079)

Biography: SUN Jing'an(1999-), male, Lianyungang, Jiangsu, Ph.D student, working on nuclear astrophysics; E-mail: [jasun22@mail.fudan.edu.cn](mailto:jasun22@mail.fudan.edu.cn)

† Corresponding author: YAN Li, E-mail: [cliyan@fudan.edu.cn](mailto:cliyan@fudan.edu.cn)

RHIC and  $|eB| \approx 10^2 m_\pi^2$  at the LHC, where  $m_\pi^2$  is the pion mass<sup>[16–19]</sup>. But the magnetic field decays drastically and is expected weak as the system starts to evolve hydrodynamically. For instance, at around 0.4 fm/c and in the center of the fireball, the residual strength of the magnetic field can drop to  $|eB| \approx 0.01 m_\pi^2$  in a non-central Au+Au collision at the top RHIC energy. Nonetheless, after the pre-equilibrium stage, the detailed evolution of the magnetic fields in QGP remains undetermined, owing to the lack of knowledge of the electrical properties of the QGP medium<sup>[20–26]</sup>.

In the scenario of a strong magnetic field, the momentum anisotropy of photons can be actually generated, relying on mechanisms such as conformal anomaly or quark transitions between Landau levels, *etc.*<sup>[27–32]</sup>. Meanwhile, the synchrotron radiation induced by a strong magnetic field presents naturally an elliptic mode<sup>[33]</sup>. However, the required magnetic field is too strong and violates the weak magnetic field fact during the hydrodynamic stage. In this paper, we obey the weak magnetic field assumption where  $|eB| \ll m_\pi^2$ . In this particular scenario, while the photon emissions within the Quark-Gluon Plasma (QGP) experience a small correction owing to the magnetic field, a substantial anisotropy in the direct photon spectrum is observed.

## 1 Method

### 1.1 The photon emission induced by weak magnetic field

The different scales of the magnetic field can modify the theoretical formalism dramatically. Especially, when  $|eB| \gg T \cdot \nabla$ , where  $\nabla$  is the space gradient, magnetohydrodynamics should be taken into account, while when  $|eB| \gg g^2 T^2$ , the quark Landau level excitations can not be neglected. In the hydrodynamic stage, the magnetic field is about  $|eB| \ll m_\pi^2$ . With such a weak magnetic field, the effect of the magnetic field should be a small correction to quark distribution. We solve the Boltzmann equation under an external magnetic field to obtain the magnetic correction,

$$f_{\text{EM}} = \frac{c}{8\alpha_{\text{EM}}} \frac{\sigma_{\text{el}} n_{\text{eq}} (1 - n_{\text{eq}})}{T^3 p \cdot u} e Q_f F^{\mu\nu} p_\mu u_\nu, \quad (1)$$

where  $eQ_f$  indicates the corresponding electrical charge a quark,  $\sigma_{\text{el}}$  is the electrical conductivity and  $u_\nu$  is flow four-velocity. Eq. (1) is consistent with the kinetic theory definition of charge current,  $j_{\text{EM}}^i = \sigma_{\text{el}} E^i = \sum_f Q_f \int \frac{d^3 p}{(2\pi)^3 p^0} p^i f_{\text{EM}}$ . The constant  $c$  is used to match this equation and the number of quark flavors. To be consistent with the perturbative photon calculations, we take the electrical conductivity as  $\sigma_{\text{el}}/T = 6$  which is also perturbative<sup>[34]</sup>.

On the other hand, photons radiated from a thermalized QGP are mainly produced by  $2 \rightarrow 2$  scattering processes among quarks and gluons ( $1 + 2 \rightarrow 3 + \gamma$ )<sup>[35]</sup>. In the kinetic theory description, the production rate is

$$\begin{aligned} \mathcal{R}^Y &= \frac{1}{2(2\pi)^3} \sum_i \int \frac{d^3 \mathbf{p}_1}{2E_1(2\pi)^3} \frac{d^3 \mathbf{p}_2}{2E_2(2\pi)^3} \frac{d^3 \mathbf{p}_3}{2E_3(2\pi)^3} \times \\ &(2\pi)^4 \delta^4(P_1 + P_2 - P_3 - P) |\mathcal{M}_i|^2 \times \\ &f_1(P_1) f_2(P_2) [1 \pm f_3(P_3)] \approx \frac{40\alpha\alpha_s}{9\pi^2} \mathcal{L} f_q(P) I_c, \quad (2) \end{aligned}$$

where the Compton and the quark-antiquark annihilation channels with respect to the scattering amplitudes  $|\mathcal{M}_i|^2$  have been summed, and  $f_1$ ,  $f_2$  and  $f_3$  are distribution functions of quarks and gluons, correspondingly. At the last line in Eq. (2), the small angle approximation is performed<sup>[36–37]</sup>, with  $\mathcal{L}$  a Coulomb logarithm, and  $I_c = \int d^3 \mathbf{p}/(2\pi)^3 [f_g + f_q]/p$  effectively characterizing the conversion between a quark-antiquark and a gluon in the thermalized QGP<sup>[38]</sup>.

After weak magnetic correction, the photon rate reads,

$$\begin{aligned} \mathcal{R}^Y &\approx \frac{40\alpha\alpha_s}{9\pi^2} \mathcal{L} [n_{\text{eq}}(P) + f_{\text{EM}}] [\bar{I}_c + I_c^{\text{EM}}] \\ &= \frac{40\alpha\alpha_s}{9\pi^2} \mathcal{L} \frac{T^2}{8} [n_{\text{eq}}(P) + f_{\text{EM}}] \\ &= \bar{\mathcal{R}}^Y + \mathcal{R}_{\text{EM}}^Y, \quad (3) \end{aligned}$$

where  $n_{\text{eq}}$  is equilibrium distribution function,  $\bar{I}_c$  is  $T^2/8$ <sup>[36]</sup> and  $I_c^{\text{EM}} = \int d^3 \mathbf{p}/(2\pi)^3 f_{\text{EM}}/p = 0$ . The  $\bar{\mathcal{R}}^Y$  represents the photon rate without magnetic contributions and the  $\mathcal{R}_{\text{EM}}^Y$  is photon radiation induced by the weak magnetic field. After a space-time integral with respect to the medium evolution, it leads to the photon invariant spectrum,

$$\begin{aligned} E_p \frac{d^3 N}{d^3 \mathbf{p}} &= \int_V \bar{\mathcal{R}}^Y(P, X) + \mathcal{R}_{\text{EM}}^Y \\ &= E_p \frac{d^3 \bar{N}}{d^3 \mathbf{p}} + E_p \frac{d^3 N_{\text{EM}}}{d^3 \mathbf{p}}. \quad (4) \end{aligned}$$

The elliptic flow of photon is defined as,

$$\begin{aligned} l v_2^Y(p_T) &= \frac{\int dy d\phi_p \cos(2\phi_p) E_p d^3 N / d^3 \mathbf{p}}{\int dy d\phi_p E_p d^3 N / d^3 \mathbf{p}} \\ &= \frac{\bar{v}_2 + \mathcal{A} v_2^{\text{EM}}}{1 + \mathcal{A}}, \quad (5) \end{aligned}$$

where,

$$\mathcal{A} = \frac{\int dy d\phi_p E_p d^3 N_{\text{EM}} / d^3 \mathbf{p}}{\int dy d\phi_p E_p d^3 \bar{N} / d^3 \mathbf{p}}, \quad (6)$$

$$v_2^{\text{EM}} = \frac{\int dy d\phi_p \cos(2\phi_p) E_p d^3 N_{\text{EM}} / d^3 \mathbf{p}}{\int dy d\phi_p E_p d^3 N_{\text{EM}} / d^3 \mathbf{p}}. \quad (7)$$

$\bar{v}_2$  is elliptic flow without magnetic correction,  $v_2^{\text{EM}}$  is

photon anisotropy induced by the magnetic field and  $\mathcal{A}$  is magnetic photon emission yield over the background photon yield, namely without magnetic correction.

## 1.2 Bjorken analysis

To explain the effect of weak magnetic photon emission from QGP, we consider the background medium in terms of the Bjorken flow, namely, a flow pattern with longitudinal expansion which is boost-invariant, and expansion in transverse directions is neglected. Written in the Milne coordinates  $(\tau, \eta_s)$ , four-momentum and the flow four-velocity are

$$p^\mu = (p_T \cosh(y - \eta_s), p_T \cos \phi_p, p_T \sin \phi_p, p_T \sinh(y - \eta_s)),$$

$$u^\mu = (1, 0, 0, 0), \quad (8)$$

where  $y$  is the rapidity and  $p_T$  the transverse momentum. Accordingly, in the presence of an external magnetic field orientated along the out-of-plane direction, the correction in the quark distribution function owing to a weak magnetic field becomes,

$$f_{\text{EM}}^{\text{Bjorken}} \propto e Q_f B_y \frac{\sinh \eta_s}{\cosh(Y - \eta_s)} n_{\text{eq}} \cos \phi_p, \quad (9)$$

where for simplicity only factors of relevance are kept.

Owing to the rapidity-odd  $v_{\text{1Ch}}^{\text{odd}}$  of the charged hadrons has been observed experimentally<sup>[39–40]</sup> and it has been captured successfully with a tilted fireball configuration<sup>[41]</sup>, one can expand the background medium as<sup>[42]</sup>,

$$n_{\text{eq}} = A_0(\tau, \eta_s, p_T, Y) + A_1(\tau, \eta_s, p_T, Y) \cos \phi_p, \quad (10)$$

where  $A_1$  is a rapidity-odd function that represents the tilted components which are responsible for  $v_{\text{1Ch}}^{\text{odd}}$ ,  $A_0$  should be an even function of rapidity as it is related to particle yields. Substitute back to Eq. (9), one has

$$f_{\text{EM}} \propto e Q B_y \frac{\sigma_{\text{el}}}{T^3} \frac{\sinh \eta_s}{\cosh(y - \eta_s)} (A_0 + A_1 \cos \phi_p) \cos \phi_p$$

$$= e Q B_y \frac{\sigma_{\text{el}}}{T^3} \frac{\sinh \eta_s}{\cosh(y - \eta_s)} \left[ \frac{A_1}{2} + A_0 \cos \phi_p + \frac{A_1}{2} \cos 2\phi_p \right]. \quad (11)$$

The term outside the brackets is an odd function of  $y$  and  $\eta_s$  and the direct photons in experiments are measured in a symmetric rapidity window,  $Y \in [-Y_M, Y_M]$ . Thus, when space-time integration is performed, only terms with rapidity-odd  $A_1$  survive and  $A_0 \cos \phi_p$  should vanish. Furthermore, Eq. (11) already implies that  $v_2^{\text{EM}} = 0.5$ . The above analysis shows that when the rapidity-odd  $v_1$  of the charged hadrons is coupled with a weak magnetic field, the elliptic flow of photons can be generated.

## 1.3 A tilted Glauber model

According to the Bjorken analysis, to get the mo-

mentum anisotropy emission of photons induced by a weak magnetic field, a tilted fireball is required to generate the rapidity-odd  $v_1$  of hadrons. Following Ref. [41], we take the initial entropy density distribution

$$s(\tau_0, \mathbf{x}_\perp, \eta_s) \propto f(\eta_s) [\chi N_{\text{coll}} + (1 - \chi) (N_{\text{part}}^+ f^+(\eta_s) + N_{\text{part}}^- f^-(\eta_s))], \quad (12)$$

where  $N_{\text{coll}}$ ,  $N_{\text{part}}^+$  and  $N_{\text{part}}^-$  are the densities of binary collisions and participants of the forward and backward going nuclei, respectively. As in the standard Glauber model, entropy production receives contributions from binary collisions and participants, relatively determined by the constant  $\chi$ . Longitudinal description in Eq. (12) is introduced via the functions  $f(\eta_s)$  and  $f^\pm(\eta_s)$ . The symmetric longitudinal profile,

$$f(\eta_s) = \exp\left(-\theta(|\eta_s| - \eta_M) \frac{(|\eta_s| - \eta_M)^2}{2\sigma_\eta^2}\right) \quad (13)$$

accounts for the longitudinal spectrum of charged hadrons, while

$$f^\pm(\eta_s) = \begin{cases} 0, & \eta_s < -\eta_T \\ \frac{\eta_T + \eta_s}{2\eta_T}, & -\eta_T \leq \eta_s \leq \eta_T \\ 1, & \eta_s > \eta_T \end{cases} \quad (14)$$

and  $f^-(\eta_s) = f^+(-\eta_s)$  give rise to rapidity-odd component. For a given collision centrality, the spatial geometry of the distribution relies entirely on these parameters,  $\eta_T$ ,  $\eta_M$ , and  $\sigma_\eta$ , which we choose as in Ref. [41]. Note, in particular,  $\eta_T$  determines the extent to which the fireball is tilted.

With this initial entropy density distribution, we solve 3+1 dimensional viscous hydrodynamics using the state-of-the-art MUSIC program<sup>[43–44]</sup>. We calculate the weak magnetic photon emission between the initial time 0.4 fm/c and an effective temperature cut  $T_c = 145$  MeV<sup>[13]</sup>.

The magnetic field is viewed as a constant in time but with  $\eta_s$  dependence as Lienard-Wiechert potential<sup>[45]</sup>,

$$eB(\eta_s) = \overline{eB} \Gamma(\tau = 0.4 \text{ fm}/c, \eta_s), \quad (15)$$

where  $\overline{eB}$  is time-averaged magnetic field strength at  $\eta_s = 0$ .

In this paper, we didn't calculate the background photon yield and elliptic flow  $\bar{v}_2$  but used the data extracted from the most updated hydrodynamical modeling in Ref. [13]. To get the elliptic flow of photon after magnetic correction in Eq. (5), we calculate the  $\mathcal{A}$  and  $v_2^{\text{EM}}$  as shown in Eqs. (6) and (7).

## 2 Results

Figure 1 shows the photon elliptic flow at RHIC 200 GeV AuAu collisions for 0~20%, 20%~40%, and 40%~60% centrality classes. The experiment data are well reproduced

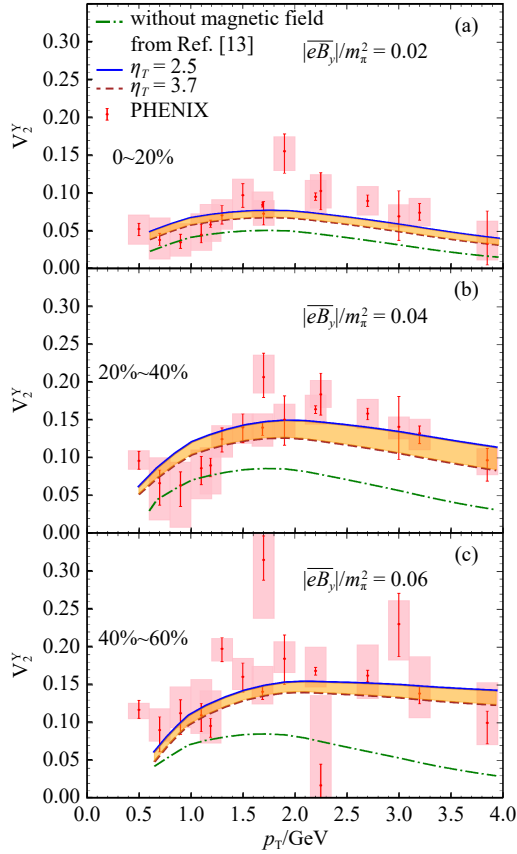


Fig. 1 The direct photon elliptic flow transverse momentum dependence at RHIC 200 GeV AuAu collisions. The green dashed line is theoretical calculations without magnetic field contribution. The blue solid line and brown dashed line are the results with weak magnetic correction but under different tilted configurations. The experiment data is from the PHENIX collaboration<sup>[9]</sup>. (color online)

for all centrality classes after weak magnetic correction. The green dashed line is the data from Ref. [13] that is  $\bar{v}_2$  without magnetic correction. The blue line is the  $v_2$  in the presence of a weak magnetic field when  $\eta_T$  is 40% of beam rapidity  $y_{\text{beam}}$ . The brown line represents  $\eta_T = y_{\text{beam}} - 2.5$ . We find that the fireball with smaller  $\eta_T$  gives a larger enhancement on the  $v_2$  under the same magnetic field. It is expected because the smaller  $\eta_T$  means the fireball is more tilted, and under the more tilted configuration the required B field is smaller to obtain the same  $v_2$  increment. As centrality grows, the time-averaged  $|\bar{eB}_y|$  systematically increases, from  $|\bar{eB}_y| = 0.02m_\pi^2$  at the 0~20% centrality class,  $|\bar{eB}_y| = 0.04m_\pi^2$  at the 20%~40% centrality class, to  $|\bar{eB}_y| = 0.06m_\pi^2$  at the 40~60% centrality class. All these values satisfy the weak magnetic field condition,  $|eB|/m_\pi^2 \ll 1$ . Weak magnetic photon emission leads to a minor increase in the direct photon yields. In the Fig. 2, the averaged yield increment is about 10% in all three centralities.

The direct photon elliptic flow is shown similarly for the PbPb collisions at  $\sqrt{s_{\text{NN}}} = 2.76$  TeV in Fig. 3. Compar-

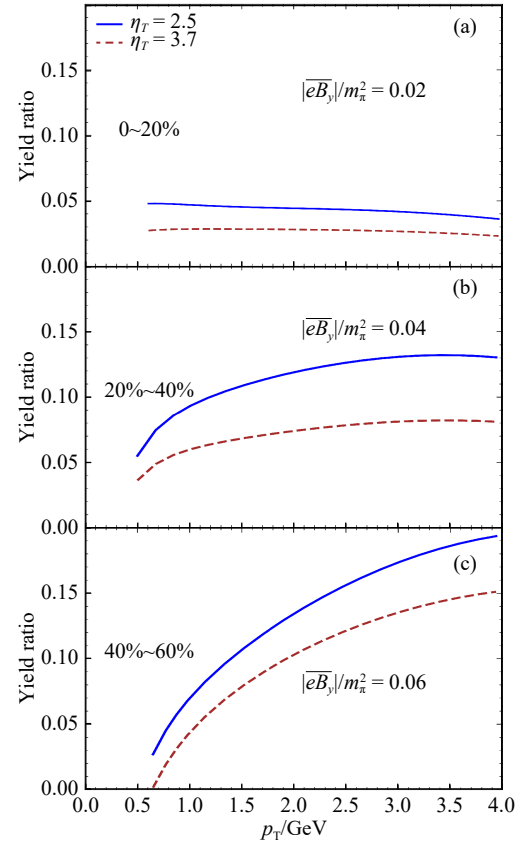


Fig. 2 The direct photon yield ratio between that with and without weak magnetic contributions transverse momentum dependence at RHIC 200 GeV AuAu collisions. The blue solid line and brown dashed line represent the different tilted configurations. (color online)

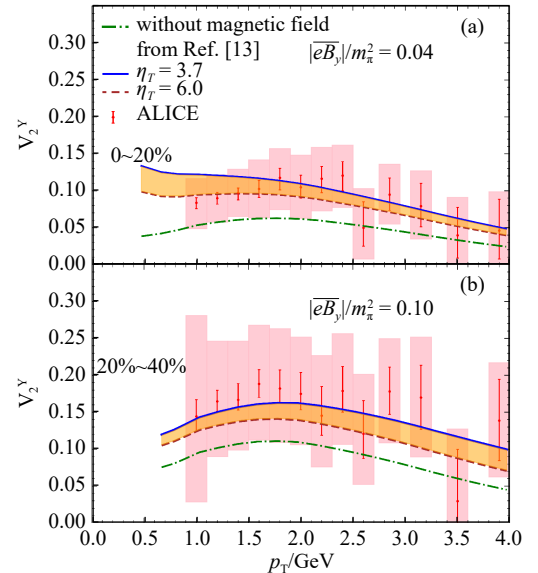


Fig. 3 The direct photon elliptic flow transverse momentum dependence at LHC 2.76 TeV PbPb collisions. The green dashed line is theoretical calculations without magnetic field contribution. The blue solid line and brown dashed line are the results with weak magnetic correction but under different tilted configurations. The experiment data is from ALICE collaboration<sup>[11]</sup>. (color online)

ing the RHIC data, there exist large experimental uncertainties from the LHC measurements. Nevertheless, with the effect of weak magnetic photon emissions, the resulting elliptic flow is improved significantly. The time-averaged  $|\overline{eB}_y^0|$  in the centrality classes 0~20% and 20%~40%, is  $0.03m_\pi^2$  and  $0.05m_\pi^2$ , respectively. Similarly, the weak magnetic field has limited contributions to the photon yield for the PbPb collisions at  $\sqrt{s_{NN}}=2.76$  TeV in Fig. 4.

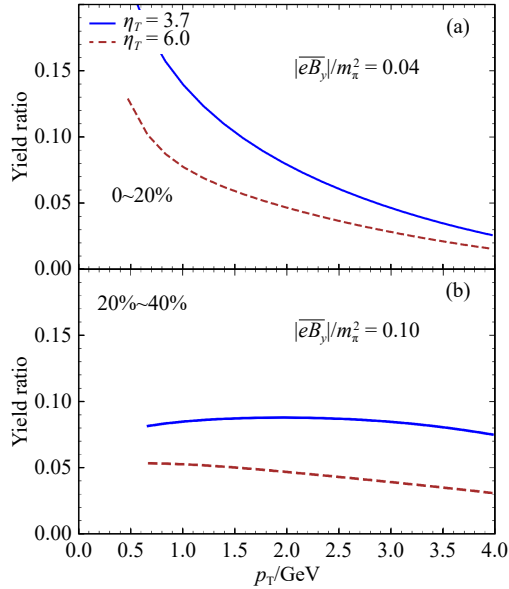


Fig. 4 The direct photon yield ratio between that with and without weak magnetic contributions transverse momentum dependence at LHC 2 760 GeV PbPb collisions. The blue solid line and brown dashed line represent the different tilted configurations. (color online)

### 3 summary

In this paper, instead of a strong magnetic field assumption which has been considered previously, we propose the effect of weak magnetic photon emission, originating from the interplay of a weak external magnetic field and the longitudinal dynamical evolution of the quark-gluon plasma. The weak magnetic photon emission results in an extra source of photon production from the quark-gluon plasma, with a large elliptic flow. In cases of Bjorken flow and more realistic 3+1D hydrodynamical evolution simulated via MUSIC, the effects of weak magnetic photon emission are justified. The experimentally measured direct photon elliptic flow at RHIC and LHC can be well reproduced. Meanwhile, the time-averaged magnetic field is still under the weak magnetic field assumption  $|eB|/m_\pi^2 \ll 1$ .

The non-trivial coupling effect between the weak magnetic field and the longitudinal dynamics of the fireball can be generalized to high-order harmonic flow. For example, the longitudinally dependent elliptic moment in QGP would generate direct photon  $v_3^{\gamma}$ , while the longitudinal dynamics of a triangular moment can contribute to  $v_4^{\gamma}$ , etc. In the fu-

ture, to explore these correlations, one needs to perform event-by-event simulations<sup>[46]</sup>. On the other hand, we are interested in the effect on other electromagnetic signals, such as local spin polarization<sup>[47]</sup> and di-lepton polarization.

The current calculation is still crude: The space-time profile of the magnetic field is simplified. Dissipations from the magnetic forces correct only the quark distribution function, while their influences on the hydrodynamic equations of motion have been neglected. Effects from the electrical field have not been taken into account. We hope we can develop a systematic hydrodynamic model incorporating the electromagnetic effect.

**Acknowledgments** We are grateful for very helpful discussions with Charles Gale, Xu-Guang Huang, Lipei Du, Kaijia Sun, and Yifeng Sun. This work is supported in part by the NSFC Grants through No. 11975079.

### References:

- [1] SHURYAK E. *Rev Mod Phys*, 2017, 89: 035001.
- [2] BUSZA W, RAJAGOPAL K, VAN DER SCHEE W. *Annual Review of Nuclear and Particle Science*, 2018, 68: 339.
- [3] GALE C, JEON S, SCHENKE B. *International Journal of Modern Physics A*, 2013, 28(11): 1340011.
- [4] SHEN C, YAN L. *Nuclear Science and Techniques*, 2020, 31(12): 122.
- [5] GALE C. *Nuclear Physics A*, 2013, 910: 147.
- [6] REYGERS K. arXiv: 2212.01220, 2022.
- [7] BLAU D, PERESUNKO D. *Particles*, 2023, 6(1): 173.
- [8] ADARE A, AFANASIEV S, AIDALA C, et al. *Phys Rev Lett*, 2012, 109: 122302.
- [9] ADARE A, AFANASIEV S, AIDALA C, et al. *Phys Rev C*, 2016, 94: 064901.
- [10] LOHNER D. *Journal of Physics: Conference Series*, 2013, 446: 012028.
- [11] ACHARYA S, ACOSTA F T, ADAMOVA D, et al. *Phys Lett B*, 2019, 789: 308.
- [12] CHATTERJEE R, SRIVASTAVA D K. *Phys Rev C*, 2009, 79: 021901.
- [13] GALE C, PAQUET J F, SCHENKE B, et al. *Phys Rev C*, 2022, 105: 014909.
- [14] SHEN C, HEINZ U, PAQUET J F, et al. *Phys Rev C*, 2015, 91(2): 024908.
- [15] PAQUET J F, SHEN C, DENICOL G S, et al. *Phys Rev C*, 2016, 93(4): 044906.
- [16] SKOKOV V, ILLARIONOV A Y, TONEEV V. *International Journal of Modern Physics A*, 2009, 24(31): 5925.
- [17] VORONYUK V, TONEEV V D, CASSING W, et al. *Phys Rev C*, 2011, 83(5): 054911.
- [18] BZDAK A, SKOKOV V. *Phys Lett B*, 2012, 710(1): 171.
- [19] DENG W T, HUANG X G. *Phys Rev C*, 2012, 85(4): 044907.
- [20] ZHANG J J, SHENG X L, PU S, et al. *Phys Rev Res*, 2022, 4: 033138.
- [21] TUCHIN K. *Phys Rev C*, 2013, 88(2): 024911.

- [22] GÜRSOY U, KHARZEEV D, RAJAGOPAL K. *Phys Rev C*, 2014, 89(5): 054905.
- [23] MCLERRAN L, SKOKOV V. *Nuclear Physics A*, 2014, 929: 184.
- [24] STEWART E, TUCHIN K. *Nuclear Physics A*, 2021, 1016: 122308.
- [25] YAN L, HUANG X G. *Phys Rev D*, 2023, 107(9): 094028.
- [26] HUANG A, SHE D, SHI S, et al. *Phys Rev C*, 2023, 107(3): 034901.
- [27] BAŞAR G, KHARZEEV D E, SKOKOV V. *Phys Rev Lett*, 2012, 109(20): 202303.
- [28] BZDAK A, SKOKOV V. *Phys Rev Lett*, 2013, 110(19): 192301.
- [29] ZAKHAROV B. *The European Physical Journal C*, 2016, 76: 1.
- [30] MÜLLER B, WU S Y, YANG D L. *Phys Rev D*, 2014, 89(2): 026013.
- [31] WANG X, SHOVKOVY I A, YU L, et al. *Phys Rev D*, 2020, 102(7): 076010.
- [32] WANG X, SHOVKOVY I. *Phys Rev D*, 2021, 104(5): 056017.
- [33] TUCHIN K. *Phys Rev C*, 2015, 91(1): 014902.
- [34] ARNOLD P B, MOORE G D, YAFFE L G. *JHEP*, 2003, 05: 051.
- [35] KAPUSTA J I, GALE C. *Finite-temperature Field Theory: Principles and Applications*[M]. Cambridge: Cambridge University Press, 2006.
- [36] BERGES J, REYGERS K, TANJI N, et al. *Phys Rev C*, 2017, 95(5): 054904.
- [37] CHURCHILL J, YAN L, JEON S, et al. *Phys Rev C*, 2021, 103(2): 024904.
- [38] BLAIZOT J P, WU B, YAN L. *Nuclear Physics A*, 2014, 930: 139.
- [39] ABELEV B, et al. *Phys Rev Lett*, 2008, 101(25): 252301.
- [40] ABELEV B, et al. *Phys Rev Lett*, 2013, 111(23): 232302.
- [41] CHATTERJEE S, BOŽEK P. *Phys Rev Lett*, 2018, 120(19): 192301.
- [42] TEANEY D, YAN L. *Phys Rev C*, 2011, 83(6): 064904.
- [43] SCHENKE B, JEON S, GALE C. *Phys Rev C*, 2010, 82(1): 014903.
- [44] SCHENKE B, JEON S, GALE C. *Phys Rev Lett*, 2011, 106(4): 042301.
- [45] HATTORI K, HUANG X G. *Nuclear Science and Techniques*, 2017, 28(2): 26.
- [46] SUN J A, YAN L. *Phys Rev C*, 2024, 109(3): 034917.
- [47] SUN J A, YAN L. arXiv: 2401.07458, 2024.

## 来自夸克-胶子等离子体的弱磁辐射

孙静安<sup>1</sup>, 严力<sup>1,2,†</sup>

(1. 复旦大学现代物理研究所, 上海 200433;  
2. 复旦大学应用离子束教育部重点实验室, 上海 200433)

**摘要:** 在相对论重离子对撞中, 必然有电磁场产生。尽管伴随夸克胶子等离子体演化的电磁场可能很弱, 但它们有可能对电磁探针有重要意义。本工作首次提出了弱磁场和背景介质的纵向动力学的耦合效应。阐明了当夸克-胶子等离子体存在弱外部磁场时, 由磁场诱导的光子是高度各向异性的。另一方面, 来自夸克-胶子等离子体的弱磁光子发射对光子产量只有很小的修正。在具有倾斜构型的火球经流体动力学演化之后, 可以很好地重现实验测量的直接光子椭圆流。同时, 在流体动力学阶段使用的时间平均磁场不大于介子质量平方的百分之几。

**关键词:** 重离子碰撞; 直接光子; 弱磁场; 椭圆流

收稿日期: 2023-06-29; 修改日期: 2024-01-06

基金项目: 国家自然科学基金资助项目 (11975079)

† 通信作者: 严力, E-mail: cliyan@fudan.edu.cn